Chemistry–A European Journal | Research Article
doi.org/10.1002/chem.202201032
Chemistry Europe
European Chemical Societies Publishing
www.chemeurj.org

Molecular Ln(III)–H–E(II) Linkages (Ln = Y, Lu; E = Ge, Sn, Pb)

Max Widemann,[a] Frederik S. W. Aicher,[a] Martin Bonath,[a] Klaus Eichele,[a] Cäcilia Maichle-Mössmer,[a] Hartmut Schubert,[a] Peter Sirsch,[a] Reiner Anwander,*[a] and Lars Wesemann*[a]

Abstract: Following the alkane-elimination route, the reaction between tetravalent aryl tintrihydride Ar*SnH_3 and trivalent rare-earth-metallocene alkyls [Cp*$_2$Ln(CH{$SiMe_3$}$_2$)] gave complexes [Cp*$_2$Ln(μ-H)$_2$SnAr*] implementing a low-valent tin hydride (Ln = Y, Lu; Ar* = 2,6-Trip$_2$$C_6H_3$, Trip = 2,4,6-triisopropylphenyl). The homologous complexes of germanium and lead, [Cp*$_2$Ln(μ-H)$_2$EAr*] (E = Ge, Pb), were accessed via addition of low-valent [(Ar*EH)$_2$] to the rare-earth-metal hydrides [(Cp*$_2$LnH)$_2$]. The lead compounds [Cp*$_2$Ln(μ-H)$_2$PbAr*] exhibit H/D exchange in reactions with deuterated solvents or dihydrogen.

Introduction

The chemistry of low-valent hydrides of the heavy Group 14 elements Ge, Sn, and Pb has been extensively studied in the past 20 years.[1] The pioneering work of P.P. Power and co-workers on low-valent dimeric hydrides of tin and germanium has emphasized the stabilizing effect of bulky terphenyl ligands.[2] In the solid state, the respective tin hydride features a hydrido-bridged dimer arrangement [Ar*Sn(μ-H)]$_2$, which in solution exhibits a dynamic interplay with the stannyl-stannylene isomer [Ar*Sn–SnH_2Ar]. The germanium hydride however shows the structure of a digermene [Ar''(H)GeGe(H)Ar''] (Ar'' = C_6H_3-2,6-Dipp$_2$, Dipp = C_6H_3-2,6-*i*Pr$_2$).[2b] Monomeric hydrides of low-valent tin and germanium were obtained in the presence of chelating ligands or bulky amides.[3] The first low-valent hydride of lead was presented five years ago, displaying the hydrido-bridged dimer motif, both in the solid state and solution.[4]

Hydride chemistry of the rare-earthmetals (Ln) is of great interest both in fundamental research and on the application side.[5] Besides the importance of parent hydride complexes, tetrahydridoborato,[6] organohydridoborato,[6f,7] and polydentate amino- or phosphinodiboranato derivatives emerged as prominent ligand classes.[8] Many of such highly reactive rare-earth-metal compounds draw on the stabilizing effect of B–H coordination.[6i,7c,9] Though of relevance for catalytic applications, the corresponding molecular Ln/Al-bimetallic hydrides have not been as well studied. In particular, Bulychev and Soloveichik have demonstrated a rich coordination chemistry of $[AlH_4]^-$, $[AlH_3]$, and $[AlH_2]^+$ moieties when introduced into rare-earth-metallocenes.[10] Piers monomeric scandium complex [LSc(AlH_4)Cl(THF)$_2$] (L = /ArNC*t*BuCHC*t*BuNAr, Ar = C_6H_3*i*Pr$_2$-2,6) revealed a 6-coordinate aluminum with three hydrido ligands bridging to the scandium center.[11] Anwander and co-workers presented the monomeric tris(pyrazolyl)borato-supported heteroaluminate complexes [Tp^{tBu,Me}Ln($HAlMe_3$)$_2$] (Ln = Y, Lu) featuring linear Ln(III)–H–Al(III) linkages.[12] The bimetallic doubly hydrido-bridged complex [Cp$_2$*Y(μ-H)$_2$Al(Me){$N(SiMe_3)_2$}] was shown to promote the hydroalumination of 1-octene.[13] f-Element silicon chemistry has revealed silanido ligands of type $[SiH_3]^-$, $[Si_2H_4]^{2-}$, $[SiH_2Ph]^-$, $[SiH(SiMe_3)_2]^-$, $[SiH_2(SiPh_3)]^-$ with predominant Ln–Si coordination[14] while Ln···H–Si β-agostic linkages are routinely observed in Ln(III) complexes with silyl-substituted amido and alkyl ligands.[15] Ln–H–E linkages involving the heavy tetrels feature the linearly aligned ytterbium complex [(Ph_3GeH)$_2$Yb(THF)$_4$] as the only example.[16] The present study reports on hydrido-bridged bimetallic complexes of the trivalent rare-earth-metals yttrium and lutetium and low-valent Group 14 elements germanium, tin, and lead.

Results and Discussion

Our initial investigations involved reaction mixtures of low-valent tin hydride [(Ar*SnH)$_2$] (**1**) and alkyl complex [Cp*$_2$Y(CH_3)(THF)] (**2**), providing evidence for hydrido-bridged complex [Cp*$_2$Y(μ-H)$_2$SnAr*] [(**3**), connectivity structure, Scheme 1]. However, side product [(Ar*$SnCH_3$)$_2$] (**4**) and reactions thereof with the tin hydride starting material (cf., Supporting Information for

[a] Dr. M. Widemann, Dr. F. S. W. Aicher, Dr. M. Bonath, Dr. K. Eichele, Dr. C. Maichle-Mössmer, Dr. H. Schubert, Dr. P. Sirsch, Prof. Dr. R. Anwander, Prof. Dr. L. Wesemann
Institut für Anorganische Chemie
Eberhard Karls Universität Tübingen
Auf der Morgenstelle 18, 72076
Tübingen (Germany)
E-mail: reiner.anwander@uni-tuebingen.de
lars.wesemann@uni-tuebingen.de

Supporting information for this article is available on the WWW under https://doi.org/10.1002/chem.202201032

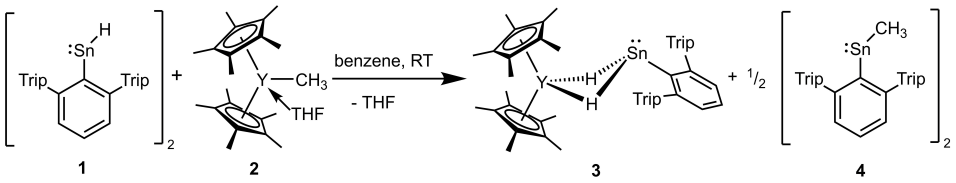

Scheme 1. Formation of the hydrido-bridged yttrium-tin compound **3**.

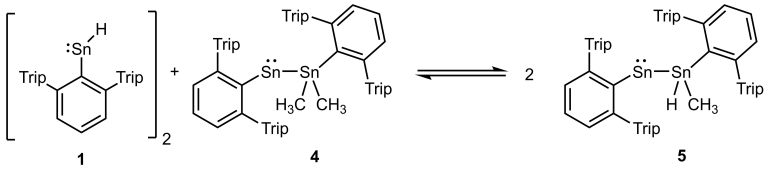

Scheme 2. Reaction of side product **4** with starting material **1**.

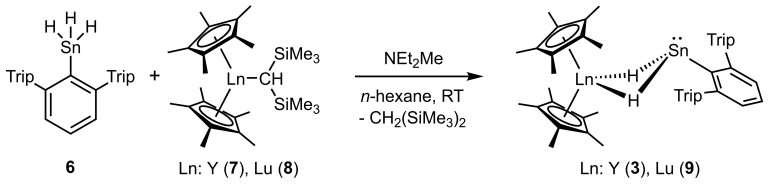

Scheme 3. Alkane-elimination route to synthesize compounds **3** and **9**.

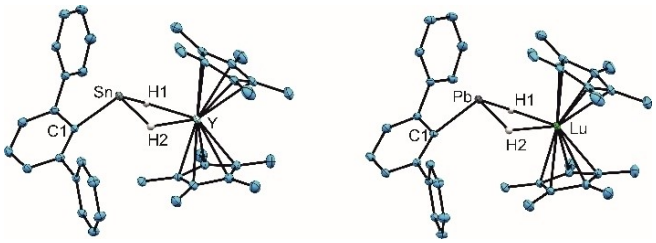

Figure 1. Crystal structures of **3** (left) and **17** (right). Atomic displacement parameters set at 50% probability. Iso-propyl groups and hydrogen atoms except for hydrido bridges are omitted for clarity. For selected interatomic distances and angles, see Table 1.

an NMR study, Scheme 2) impeded the isolation of **3**. Therefore, we envisaged different synthesis protocols.

Treatment of the donor-free alkyl complexes [$Cp^*_2Ln(CH\{SiMe_3\}_2)$] (Ln = Y (**7**), Lu (**8**)) with organotin(IV) trihydride [Ar^*SnH_3] (**6**) in the presence of diethyl methylamine resulted in alkane elimination and the formation of bimetallic complexes [$Cp^*_2Ln(\mu\text{-}H)_2SnAr^*$] (Ln = Y (**3**), Lu (**9**)) (Scheme 3). Base NEt_2Me has shown previously to trigger dihydrogen elimination in organotin trihydrides.[17] Both stannylene hydride complexes were obtained in reasonable yield (**3**: 87%, **9**: 68%). The molecular structure of the yttrium derivative **3** is depicted in Figure 1 (**9**: Figure S1) and selected interatomic distances are listed in Table 1. Selected NMR data of complexes **3** and **9** are

Table 1. Selected interatomic distances [Å] and angles [deg] for complexes **3**, **9**, **15**, **16**, and **17**.

Ln–E	Y–Sn (**3**)	Y–Pb (**16**)	Lu–Ge (**15**)[a]	Lu–Sn (**9**)	Lu–Pb (**17**)
Ln–E	3.2374(5)	3.2957(4)	2.77	3.1868(4)	3.2441(2)
Ln–H	2.27(3), 2.25(3)	2.23(4), 2.20(4)		2.17(4), 2.20(5)	2.25(5), 2.19(4)
E–H	1.84(3), 1.85(3)	1.93(4), 1.95(4)		1.82(4), 1.91(4)	1.87(5), 1.95(4)
E–C1	2.244(2)	2.340(3)	2.01	2.251(3)	2.344(3)
Ln–Cp*	2.600(3)–2.666(3)	2.602(3)–2.674(4)	2.55–2.60	2.552(3)–2.626(3)	2.557(3)–2.628(3)
Ln–E–C1	122.2(1)	120.8(1)		121.6(1)	120.8(1)
H1–Ln–H2	63.2(1)	66.7(14)		65.1(16)	66.1(16)
H1–E–H2	79.9(2)	77.8(17)		78.2(19)	79(2)
C1-E–H1	98.6 (10)	103.3(13)		100.1(12)	98.3(14)
C1–E–H2	104.8(11)	105.1(12)		104.2(14)	105.6(13)
Ln–H1–E	103.1(1)	103.7(8)		105.8(9)	103.7(4)
Ln–H2–E	104.4(2)	104.8(2)		101.8(4)	103.0(2)
Σ E[b]	283	286		293	283

[a] **15** exhibits a slight disorder in the solid state. Hydrogen atoms were placed in calculated positions. [b] Sum of angles around atom E.

compiled in Table 2. The less reactive germanium trihydride Ar*GeH_3 did not engage in alkane elimination with [Cp*$_2$Ln(CH{$SiMe_3$}$_2$)] and the analogous lead trihydride Ar*PbH_3 is unknown.[18] Therefore, we targeted addition reactions of the low-valent hydrides [(Ar*EH)$_2$] [E = Ge (**10**),[2b,19] Pb (**11**)[4a,b]] to the rare-earth-metal hydrides [(Cp*$_2$Ln(μ-H)$_2$] [Ln = Y (**12**), Lu (**13**)[20]] (Scheme 4). A similar procedure was employed by Evans and co-workers for the synthesis of [Cp*$_2$Y(μ-H)$_2$$BC_8H_{14}$].[7g] The bimetallic hydrido-bridged complexes [Cp*$_2$Ln(μ-H)$_2$EAr*] [Y/Ge **14** (47%), Lu/Ge **15** (41%), Y/Pb **16** (61%), Lu/Pb **17** (52%)] were obtained as yellow (**14**, **15**, **17**) or orange (**16**) colored solids. Crystals suitable for XRD analysis were obtained from solutions in *n*-pentane (Lu/Pb **17**, Figure 1; for the crystal structures of **9**, **15**, **16** see Supporting Information). The presented bimetallic rare-earth-metal complexes are moisture- and temperature-sensitive and were stored at −40 °C under argon.

Comparing the interatomic distances found in the solid-state structures of **3**, **9**, **15**–**17**, as expected the smaller lutetium atom exhibits shorter distances than yttrium. Furthermore, the series of Ln/E compounds seemed to indicate a comparatively short Ln–Ge distance, although a slight disorder of the germanium atom over two positions precludes any further interpretation. Ln–H–Ge linkages were only reported for the aforementioned ytterbium complex [(Ph_3GeH)$_2$Yb(THF)$_4$].[16] Direct Ln–Ge and Ln–Sn linkages were also mainly described for divalent Ln(II) (Ln = Eu, Sm, Yb)[14a] involving anionic ligands of type R_3E [E = Ge, Sn, R = Ph;[21] E = Sn, R = Me_3Sn,[22] CH_2tBu,[23] (2-pyridyl)[24]], chelating (Ph_2Ge)$_4$,[25] and metalloid cluster [Ge_9{Si($SiMe_3$)$_3$}$_3$].[26] Dysprosium complexes [(C_5H_4iPr)$_2$Dy($GePh_3$)(THF)] and [(C_5Me_5)$_2$Dy($SnPh_3$)(THF)] display rare examples of Ln(III)/heavy tetrel bonding and were accessed both via salt metathesis and alkane-elimination protocols, respectively.[21d] Hydrido-bridged lanthanide complexes with low-valent element hydrides have not been reported so far.

In the IR spectra, bands for the Ln-(μ-H)$_2$-E moiety could not be clearly assigned because they are obscured by vibrations of the other ligands. However, based on the IR data of bridged hydrides [(Ar*PbH)$_2$],[4a] [(Ar*SnH)$_2$],[2c] [HPb(μ-H)]$_2$,[27] [Cp_2Lu(μ-H)AlH_3(NEt_3)][10b] the bands for Ln-(μ-H)$_2$-E should appear in the 800–1200 cm^{-1} range. The NMR spectroscopy studies confirm the molecular structures found in the solid state. In the series of Group 14 elements Ge, Sn, and Pb the signal in the ^{1}H NMR spectrum of the hydrido ligands was found at increasing frequency ($\Delta\delta$ = 10.17–10.52 ppm). Whereas the influence of the different rare-earth metals Y and Lu is in the series of compounds much smaller ($\Delta\delta$ = 0.32–1.01 ppm). The lead hydride resonances of **16** and **17** at high frequency are a result of the spin-orbit coupling between the lead and hydrogen atom (SO-HALA effect). The SO-HALA effect, which was intensively studied,[28] is very pronounced in the case of the low valent hydrides [(Ar*EH)$_2$] (E = Ge, 6.30 ppm,[2b] E = Sn, 7.87/9.82 ppm),[2a] E = Pb, 35.61 ppm).[4a] The ^{119}Sn NMR signals of **3** and **9** lie in the typical range for triply coordinate Sn(II) compounds and can be compared with low-valent tin adducts [Ar*SnH(^{Et}NHC)] (−338 ppm),[29] [(DipNacNac)SnH)] (−225 ppm),[3d] and [Ar*SnH(DMAP)] (225 ppm).[17c] The size of the Sn–H coupling constant (Table 2) points to a small s-orbital participation, which is an argument for a lone pair on the tin atom corroborating the trigonal pyramidal coordination (see Table 1 sum of angles around Sn). These findings are in line with the lithium/tin hydrido-bridged dimer [(TMPDA)Li(μ-H)$_2$SnAr*] ($^1J_{Sn-H}$ = 175 Hz).[19] The ^{207}Pb NMR signals of **16** and **17** can be compared with the ^{207}Pb NMR signal found for the hydride [(Ar*PbH)$_2$] (3736 ppm)[4b] and range at low frequencies in comparison to the rhodium derivative [(Ph_3P)$_2$Rh(μ-H)$_2$PbAr*] (8195 ppm).[30] The $^1J_{Pb-H}$ coupling constants observed for **16** (1090 Hz) and **17** (1069 Hz) are large in comparison to other low valent lead hydride coupling constants: [(ArPbH)$_2$] (Ar = Ar*, Ar', Ar^{iPri4}, 696–734 Hz),[4] [Ar*PbH(^{Me}NHC)] (955 Hz),[4a] [(Ph_3P)$_2$Rh(μ-

Table 2. NMR data of complexes **3**, **9**, and **14**–**17**.

Ln–H–E	^{1}H NMR δ [ppm]	$^1J_{E-H}$ [Hz] E = ^{119}Sn/^{207}Pb	$^1J_{Y-H}$ [Hz]	^{119}Sn/^{207}Pb NMR δ [ppm]	^{89}Y NMR δ [ppm] (J_{E-Y}) [Hz]
Y–Ge (**14**)	3.64		7.4		105
Lu–Ge (**15**)	4.31				
Y–Sn (**3**)	4.83	148	19.3	−36	65 (85)
Lu–Sn (**9**)	5.84	228		−54	
Y–Pb (**16**)	14.16	1090	22.0	2261	173 (386)
Lu–Pb (**17**)	14.48	1069		2251	

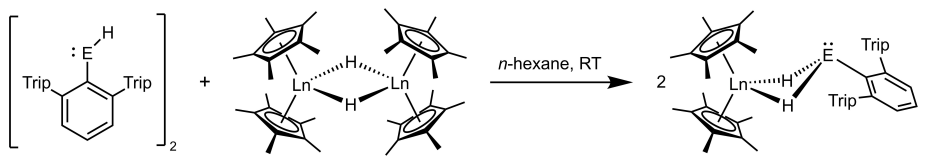

E: Ge (**10**), Pb (**11**)

Ln: Y (**12**), Lu (**13**)

E: Ge, Ln: Y (**14**)
E: Ge, Ln: Lu (**15**)
E: Pb, Ln: Y (**16**)
E: Pb, Ln: Lu (**17**)

Scheme 4. Exchange between hydrido-bridged dimers.

H)$_2$PbAr*] (124 Hz) (Ar′ = 2,6-Mes$_2$C$_6$H$_3$, Mes = 2,4,6-trimethylphenyl; Ar^{iPr4} = C$_6$H$_3$-2,6-(C$_6$H$_3$-2,6-^{i}Pr$_2$)$_2$).[30] Due to the coupling with the protons and the ^{89}Y isotope (100%, I = 1/2), the ^{119}Sn (**3**) and ^{207}Pb NMR spectra (**16**) show a doublet of triplets. The signals in the ^{89}Y NMR spectra of **3**, **14**, and **16** were found in the range of Cp*$_2$YR complexes.[6h,31] The $^1J_{Y\text{-}H}$ coupling constants, which were observed in the ^{1}H NMR spectra of **14** (Y–Ge, 7.4 Hz), **3** (Y–Sn, 19.3 Hz), and **16** (Y–Pb, 22.0 Hz), can be compared with hydrido-bridged yttrium complexes [(Cp*$_2$Y μ-H)$_2$] (37.5 Hz),[32] [Cp*Y(μ-H){μ-η^5,η^1(C$_5$Me$_4$CH$_2$}YCp*$_2$][33] and [Cp*$_2$Y(μ-H)$_2$Al(Me){N(SiMe$_3$)$_2$}] (20.5–25.5 Hz).[6h,34] The $^1J_{Y\text{-}H}$ coupling constant for the germanium derivative is considerably smaller than those detected in the tin and lead derivatives. This observation might indicate a slight change of the [Y(μ-H)$_2$E] coordination. For comparison, the TMPDA–Li-salts of anions [Ar*EH$_2$]$^-$ (E = Ge, Sn) revealed two different coordination modes arising from distinct tetrel nucleophilicities (Ge > Sn) (Scheme 5).[19] Accordingly, we assumed a higher degree of Y–Ge bond formation in [Cp*$_2$Y(μ-H)$_2$GeAr*] (Scheme 5), which would be in line with a reduction of the Y–H interaction. Bochkarev et al. discussed a comparable situation with the coordination of Ph$_3$GeH at ytterbium in [(Ph$_3$GeH)$_2$Yb(THF)$_4$].[16] To correlate our spectroscopic findings with the electronic situation, quantum chemical calculations were carried out using ORCA.[35] The geometries of all bimetallic complexes were optimized, including **14**, for which a crystal structure could not be obtained. The calculated structural parameters for **3**, **9**, **16**, and **17** were in good agreement with their X-ray counterparts reported above (for details, see the Supporting Information). The calculated Y–H distances for **3**, **14**, and **16** were in a similar range, but showed a slight trend toward increasing distances in the series E = Pb (2.17 Å), Sn (2.19 Å), Ge (2.22 Å avg.). A similar trend could be observed for the corresponding Lu–H distances in **9**, **15**, and **17**. Due to these small differences, we carried out an NBO analysis to explore the bonding in more detail.[36] The data revealed that for all complexes, both the lone pair on E and the E–H bonds donate electron density toward the rare-earth metal, which supports the view of an intermediate coordination mode, as depicted in Scheme 5. Within the NBO scheme, these contributions can be quantified by analyzing the atomic composition of the respective natural localized molecular orbitals (NLMOs), which represent the parent Lewis-type NBOs (lone pair on E, E–H bonds), along with their non-Lewis delocalization tails, which originate from donor-acceptor interactions, for example, toward the rare-earth metal. In the case of the complexes featuring yttrium, the rare-earthmetal atom shares an increasing amount of electron density, associated with the lone pair on E, when going from E = Pb (3.8%) and Sn (5.0%) to its lighter congener Ge (7.4%). At the same time, the E–H–Y interaction noticeably decreases, as indicated by the atomic contributions of Y to the NLMOs associated with the E–H bonds (E = Pb: 10.6/11.2%; E = Sn: 9.5/9.8%; E = Ge: 7.5/7.7%). An analogous trend was observed for the complexes containing lutetium. Both types of NLMOs are displayed in Figure 2 for the case of **14**.

Finally, it is also noteworthy to mention, that the NBO-derived atomic charges on the bridging hydrido ligands, *q*(H), change significantly, when germanium is involved, due to the smaller bond polarity of the Ge–H bond: *q*(H) = −0.23 (E = Ge) vs. −0.38 and −0.40, in the case of Sn and Pb, respectively. This might also be a contributing factor to the observed differences in the $^1J_{Ln\text{-}H}$ coupling constant.

Solutions of the lead derivatives **16** and **17** in aromatic solvents show formation of the diplumbyne [(Ar*Pb)$_2$], which was also found as the product of lead hydride [(Ar*PbH)$_2$] decomposition (complete decomposition after 2.5 h, RT). The yttrium complex (14 h, RT, 16% decomposition) shows a much faster decomposition reaction in comparison to the lutetium complex (14 h, RT, 9% decomposition). Besides decomposition both complexes show an H/D-exchange reaction in benzene-d$_6$ solution at ambient temperature. A mixture of (μ-H)$_2$/(μ-H)(μ-D) species of 60:40% was observed after 1 h in the ^{1}H NMR spectrum, with the Y/Pb complex, and after 5 h with the Lu/Pb compound. Rare-earth-metal hydrides [(Cp*$_2$LnH)$_2$] are well known for their H/D exchange reactivity via σ-bond metathesis.[20,32,37] The completely deuterated complex of **16** could be transferred back to the hydrogenated species via reaction with C$_6$H$_6$ or H$_2$. The slightly larger yttrium ion exhibits higher reactivity in both reactions, decomposition and H/D exchange. The ^{207}Pb NMR spectrum of the deuterated complex [Cp*$_2$Y(D)$_2$PbAr*] revealed a signal at a smaller frequency (2229 ppm, $^1J_{Pb\text{-}D}$ = 167 Hz, $^2J_{Pb\text{-}Y}$ = 387 Hz) in comparison to the hydrogen species **16** (2261 ppm, d/tr, $^1J_{Pb\text{-}H}$ = 1090 Hz, $^2J_{Pb\text{-}Y}$ = 386 Hz). The ratio of the Pb–D/Pb–H coupling constants is in agreement with the ratio of magnetogyric ratios, γ(^{2}H)/γ(^{1}H). The ^{207}Pb isotope shift difference of Pb(H)$_2$Y versus Pb(D)$_2$Y species of $\Delta\delta$ = −32 ppm was predicted by Jameson and

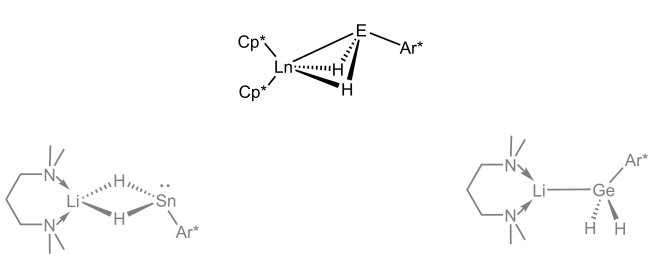

Scheme 5. Coordination geometry for the hydrido-bridged bimetallic complexes reported in this work (Ln = Y, Lu; E = Ge, Sn, Pb), in comparison to related Li salts with low-valent Group 14 element hydrides.[19]

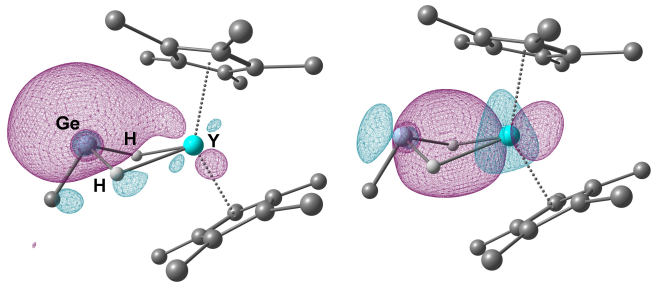

Figure 2. Depiction of the NLMOs in **14**, which represent the donor-acceptor interactions between Y and the lone pair on Ge (left) and one of the Ge–H bonds (right), respectively.

coworkers.[38] The homologous tin derivatives **3** and **9** show less pronounced H/D exchange reactivity: after several hours at 50 °C only a small amount (< 5 %) of deuterated product was found in the NMR spectra. The germanium derivatives **14** and **15** do not show any H/D exchange activity in solution at ambient temperature.

Conclusion

Hydrido-bridged bimetallic complexes featuring trivalent rare-earth-metals yttrium and lutetium and divalent heavy Group 14 elements germanium, tin, and lead are accessible via the alkane-elimination route or an element-hydride exchange reaction. In particular, molecular Ln–H–Sn linkages bear relevance to organolanthanide-promoted hydrostannylation reactions.[39]

Experimental Section

General remarks: General information. All manipulations were carried out under an argon atmosphere using standard Schlenk techniques and gloveboxes. *n*-Pentane and *n*-hexane were dried using a M. Braun – Solvent Purification System (SPS). All solvents were distilled from sodium or potassium. All solvents were subsequently degassed by 3×freeze/pump/thaw. [(2,6-$Trip_2C_6H_3SnH)_2$],[2a] [2,6-$Trip_2C_6H_3SnH_3$],[40] [(2,6-$Trip_2C_6H_3PbH)_2$],[4a,b] [$Cp^*_2YCH(SiMe_3)_2$],[41] [$Cp^*_2LuCH(SiMe_3)_2$],[20] [$(Cp^*_2YH)_2$],[37a] [$(Cp^*_2LuH)_2$][20] were synthesized following literature procedures. [$(Ar^*GeH)_2$] was synthesized by treatment of [$(Ar^*GeCl)_2$] with [Ar^*GeH_2][$Li((thf)_3$].[19,42] Further chemicals were purchased commercially and used as received. Elemental analyses were performed at the Institute of Inorganic Chemistry, University of Tübingen using a Vario MICRO EL analyzer.

NMR spectroscopy: NMR spectra were recorded with either a Bruker Avance III HD 300 NanoBay spectrometer equipped with a 5 mm BBFO probe head and operating at 300.13 (^{1}H), 75.47 (^{13}C), 111.92 (^{119}Sn), and 62.79 MHz (^{207}Pb), a Bruker AvanceII + 400 NMR spectrometer equipped with a 5 mm QNP (quad nucleus probe) head and operating at 400.11 (^{1}H), 100.62 MHz (^{13}C), a Bruker AVII + 500 NMR spectrometer with a variable temperature set up and a 5 mm TBO probe head and operating at 500.13 (^{1}H), 125.76 (^{13}C) and 104.63 MHz (^{207}Pb), a Bruker Avance III HDX 600 NMR spectrometer with a 5 mm Prodigy BBO cryo probe head operating at 600.13 (^{1}H) and 150.90 (^{13}C) MHz or a Bruker Avance III HDX 700 NMR spectrometer with a 5 mm Prodigy TCI cryo probe head operating at 700.29 (^{1}H) and 176.10 MHz (^{13}C). Chemical shifts are reported in δ values in ppm relative to external TMS (^{1}H, ^{13}C), $SnMe_4$ (^{119}Sn) or $PbMe_4$ (^{207}Pb) referenced in most cases on the residual proton signal of the solvent C_6D_6 (^{1}H 7.15 ppm; ^{13}C 128.0 ppm). ^{1}H and ^{13}C-spectra in toluene-d_8, benzene-d_6 were referenced using the chemical shift of the solvent ^{2}H resonance frequency and Ξ = 25.145020 % for ^{13}C, Ξ = 37.290632 % for ^{119}Sn and Ξ = 20.920599 % for ^{207}Pb.[43] The multiplicity of the signals is abbreviated as s = singlet, d = doublet, t = triplet, quint = quintet, sept = septet and m = multiplet or unresolved. The proton and carbon signals were assigned by detailed analysis of ^{1}H, ^{13}C {^{1}H}, ^{1}H-^{1}H COSY, ^{1}H-^{13}C HSQC, ^{1}H-^{13}C HMBC and ^{13}C{^{1}H} DEPT-135 spectra. ^{1}H-^{89}Y-HSQC NMR experiments were performed on a Bruker AVII + 500 NMR spectrometer using 5 mm tubes with a 5 mm ATM probehead operating at 500.13 (^{1}H) and 24.51 MHz (^{89}Y). For ^{89}Y NMR the IUPAC reference standard with Ξ = 4.900198 % has been used.[43]

Crystallography: X-ray data were collected with a Bruker Smart APEX II diffractometer with graphite-monochromated Mo K_α radiation or a Bruker APEX II Duo diffractometer with a Mo IμS microfocus tube. The programs used were Bruker's APEX2 v2011.8-0, including SAINT for data reduction. SADABS for absorption correction, and SHELXS for structure solution, as well as the WinGX suite of programs version 1.70.01 or the GUI ShelXle, including SHELXL for structure refinement.[44]

Quantum chemical calculations: On the basis of the molecular structures of **3**, **9**, **15**, **16**, **17**, determined in the solid state, and in the case of **14**, based on the molecular structure of **3** (while Sn was exchanged for Ge), the geometries of the bimetallic complexes were optimized using the programme Orca4.2.1[35] along with BP86,[45] Grimme's dispersion correction and Becke-Johnson damping (D3BJ).[46] The basis sets employed were def2-TZVP for Ge, Sn, Pb, Y, Lu (in combination with def2 effective core potentials, except for Ge), as implemented in ORCA4.2.1, and def2-SVP on all other elements.[47] For all calculations, tight or very tight convergence criteria were applied for optimizations and SCF convergence, respectively; as gridsizes "grid6" and "finalgrid7" were selected. Absence of imaginary frequencies on this level of theory confirmed local minima on the PES. Analyses of the electronic structures were performed using NBO7, plots were generated using Chemcraft.[36,48]

The data that support the findings of this study are available in the Supporting Information for this article.

Synthesis: Synthesis of $Cp^*_2Y(\mu\text{-}H)_2SnAr^*$ (**3**). $Cp^*_2YCH(SiMe_3)_2$ (60.0 mg, 116 μmol, 1.00 eq.) and Ar^*SnH_3 (69.8 mg, 116 μmol, 1.00 eq.) were suspended in *n*-pentane (2.5 mL) and NEt_2Me (ca. 50 μL, ca. 36 mg, ca. 400 μmol, ca. 4 eq.) was added. The reaction mixture was stirred in a closed reaction vessel for 24 h at ambient temperature, upon which it turned into a yellow suspension. Filtration of the yellow solid, additional washing with *n*-pentane (1×1 mL) and drying *in vacuo* yielded the product $Cp^*_2Y(\mu\text{-}H)_2SnAr^*$ as yellow powder (96.8 mg, 101 μmol, 87 %). Crystals suitable for X-ray analysis could be obtained from a saturated pentane solution after several days at ambient temperature. **Elemental analysis** calcd (%) for $C_{56}H_{81}SnY$: C 69.93, H 8.49; found: C 70.02, H 8.41.

Synthesis of $Cp^*_2Lu(\mu\text{-}H)_2SnAr^*$ (**9**). $Cp^*_2LuCH(SiMe_3)_2$ (30.0 mg, 49.6 μmol, 1.00 eq.) and Ar^*SnH_3 (29.9 mg, 49.6 μmol, 1.00 eq.) were suspended in *n*-pentane (1 mL) and NEt_2Me (ca. 25 μl, ca. 20 mg, ca. 200 μmol, ca. 4 eq.) was added. The reaction mixture was stirred in a closed reaction vessel for 48 h at ambient temperature, upon which it turned into a yellow suspension. Filtration of the yellow solid, additional washing with *n*-pentane (1×0.5 mL) and drying *in vacuo* yielded the product $Cp^*_2Lu(\mu\text{-}H)_2SnAr^*$ as yellow powder (35.1 mg, 33.5 μmol, 68 %). Crystals suitable for X-ray analysis could be obtained from a saturated *n*-pentane solution after several days at ambient temperature. **Elemental analysis** calcd (%) for $C_{56}H_{81}LuSn$: C 64.18, H 7.79; found: C 64.22, H 7.82.

Synthesis of $Cp^*_2Y(\mu\text{-}H)_2PbAr^*$ (**16**). $[Cp^*_2YH]_2$ (20.0 mg, 27.7 μmol, 1.00 eq.) and $[Ar^*PbH]_2$ (38.3 mg, 27.7 μmol, 1.00 eq.) were suspended in *n*-pentane (1.5 mL) and stirred in a closed reaction vessel for 20 h at ambient temperature. Filtration of the orange solid, additional washing with pentane (1×0.5 mL) and drying *in vacuo* yielded the crude product. Redissolving it in benzene (or C_6D_6) led to a blackish-yellow suspension, which after filtration through a syringe filter, to remove elemental lead, yielded a clear, yellow solution of the product $Cp^*_2Y(\mu\text{-}H)_2PbAr^*$. Attempts to remove the solvent again *in vacuo* resulted in a deep red coloration of the reaction solution. However, a satisfactory elemental analysis could be obtained from the red residue (35.6 mg, 33.9 μmol, 61 %). Also, under 1 atm argon the solution at ambient temperature tended to a slow orange-red coloration with loss of H_2 and formation of,

among others, [Ar*PbPbAr*]. Crystals suitable for X-ray analysis could be obtained from a saturated *n*-pentane solution after several days at −40 °C. **Elemental analysis** calcd (%) for $C_{56}H_{81}PbY$: C 64.04, H 7.77; found: C 64.47, H 7.57.

Synthesis of $Cp^*_2Lu(\mu\text{-}H)_2PbAr^*$ (**17**). $[Cp^*_2LuH]_2$ (28.0 mg, 31.4 μmol, 1.00 eq.) and $[Ar^*PbH]_2$ (43.3 mg, 31.4 μmol, 1.00 eq.) were suspended in *n*-pentane (1.5 mL) and stirred in a closed reaction vessel for 20 h at ambient temperature. All volatiles were removed *in vacuo*, benzene (2 mL) were added and the solution stirred for 5 h. After filtration through a syringe filter the solvent was again removed *in vacuo* and the residue resuspended in *n*-pentane (1.5 mL). Vigorous stirring for 15 min led to a yellow-orange suspension. Filtration of the yellow solid, additional washing with *n*-pentane (1×0.5 mL) and drying *in vacuo* yielded the product $Cp^*_2Lu(\mu\text{-}H)_2PbAr^*$ as yellow powder (37.2 mg, 32.7 μmol, 52%). Crystals suitable for X-ray analysis could be obtained from a saturated *n*-pentane solution after several days at ambient temperature. **Elemental analysis** calcd (%) for $C_{56}H_{81}LuPb$: C 59.19, H 7.18; found: C 58.73, H 7.05.

Synthesis of $Cp^*_2Y(\mu\text{-}H)_2GeAr^*$ (**14**). $[Cp^*_2YH]_2$ (20.8 mg, 28.9 μmol, 1.00 eq.) and $[Ar^*GeH]_2$ (32.1 mg, 28.9 μmol, 1.00 eq.) were suspended in *n*-pentane (2.5 mL) and stirred for 3 days at ambient temperature. All volatiles were removed *in vacuo*, benzene (3 mL) were added and the suspension filtered through a syringe filter. The solvent was again removed *in vacuo* and the light yellow residue resuspended in *n*-pentane (1.5 mL). Vigorous stirring for 15 min led to a yellow suspension. Filtration of the solid, additional washing with *n*-pentane (1×0.5 mL) and drying *in vacuo* yielded the product $Cp^*_2Y(\mu\text{-}H)_2GeAr^*$ as light yellow powder (24.9 mg, 27.2 μmol, 47%). **Elemental analysis** calcd (%) for $C_{56}H_{81}GeY$: C 73.45, H 8.92; found: C 73.44, H 8.59.

Synthesis of $Cp^*_2Lu(\mu\text{-}H)_2GeAr^*$ (**15**). $[Cp^*_2LuH]_2$ (30.5 mg, 34.1 μmol, 1.00 eq.) and $[Ar^*GeH]_2$ (37.9 mg, 34.1 μmol, 1.00 eq.) were suspended in *n*-pentane (2.5 mL) and stirred for 3 days at ambient temperature. All volatiles were removed *in vacuo*, benzene (3 mL) were added and the suspension filtered through a syringe filter. The solvent was again removed *in vacuo* and the light yellow residue resuspended in *n*-pentane (2 mL). Vigorous stirring for 15 min led to a yellow suspension. Filtration of the solid, additional washing with *n*-pentane (1×0.5 mL) and drying *in vacuo* yielded the product $Cp^*_2Lu(\mu\text{-}H)_2GeAr^*$ as light yellow powder (27.7 mg, 27.6 μmol, 41%). Crystals suitable for X-ray analysis could be obtained from a saturated pentane solution after several days at ambient temperature. **Elemental analysis** calcd (%) for $C_{56}H_{81}GeLu$: C 67.14, H 8.15; found: C 67.16, H 7.97.

Deposition Number(s) 2162810 (for **16**), 2162811 (for **3**), 2162812 (for **9**), 2162813 (for **17**), and 2162814 (for **15**) contain the supplementary crystallographic data for this paper. These data are provided free of charge by the joint Cambridge Crystallographic Data Centre and Fachinformationszentrum Karlsruhe Access Structures service.

Acknowledgements

We acknowledge support of the state of Baden-Württemberg through bwHPC and the German research Foundation (DFG) through grant no INST 40/575-1 FUGG (Justus 2 cluster), and WE 1876/13-1. Open Access funding enabled and organized by Projekt DEAL.

Conflict of Interest

The authors declare no conflict of interest.

Data Availability Statement

The data that support the findings of this study are available in the supplementary material of this article.

Keywords: germanium · hydride · lanthanide · lead · tin

[1] a) M. M. D. Roy, A. A. Omaña, A. S. S. Wilson, M. S. Hill, S. Aldridge, E. Rivard, *Chem. Rev.* **2021**, *121*, 12784–12965; b) T. J. Hadlington, M. Driess, C. Jones, *Chem. Soc. Rev.* **2018**, *47*, 4176–4197; c) E. Rivard, *Chem. Soc. Rev.* **2016**, *45*, 989–1003; d) E. Rivard, P. P. Power, *Dalton Trans.* **2008**, 4336–4343.
[2] a) B. E. Eichler, P. P. Power, *J. Am. Chem. Soc.* **2000**, *122*, 8785–8786; b) A. F. Richards, A. D. Phillips, M. M. Olmstead, P. P. Power, *J. Am. Chem. Soc.* **2003**, *125*, 3204–3205; c) E. Rivard, R. C. Fischer, R. Wolf, Y. Peng, W. A. Merrill, N. D. Schley, Z. Zhu, L. Pu, J. C. Fettinger, S. J. Teat, I. Nowik, R. H. Herber, N. Takagi, S. Nagase, P. P. Power, *J. Am. Chem. Soc.* **2007**, *129*, 16197–16208.
[3] a) S. K. Mandal, H. W. Roesky, *Acc. Chem. Res.* **2012**, *45*, 298–307; b) A. Jana, H. W. Roesky, C. Schulzke, A. Döring, *Angew. Chem. Int. Ed.* **2009**, *48*, 1106–1109; *Angew. Chem.* **2009**, *121*, 1126–1129; c) A. Jana, D. Ghoshal, H. W. Roesky, I. Objartel, G. Schwab, D. Stalke, *J. Am. Chem. Soc.* **2009**, *131*, 1288–1293; d) L. W. Pineda, V. Jancik, K. Starke, R. B. Oswald, H. W. Roesky, *Angew. Chem. Int. Ed.* **2006**, *45*, 2602–2605; *Angew. Chem.* **2006**, *118*, 2664–2667; e) T. J. Hadlington, B. Schwarze, E. I. Izgorodina, C. Jones, *Chem. Commun.* **2015**, *51*, 6854–6857; f) T. J. Hadlington, M. Hermann, G. Frenking, C. Jones, *Chem. Sci.* **2015**, *6*, 7249–7257; g) T. J. Hadlington, M. Hermann, G. Frenking, C. Jones, *J. Am. Chem. Soc.* **2014**, *136*, 3028–3031; h) T. J. Hadlington, M. Hermann, J. Li, G. Frenking, C. Jones, *Angew. Chem. Int. Ed.* **2013**, *52*, 10199–10203; *Angew. Chem.* **2013**, *125*, 10389–10393.
[4] a) J. Schneider, C. P. Sindlinger, K. Eichele, H. Schubert, L. Wesemann, *J. Am. Chem. Soc.* **2017**, *139*, 6542–6545; b) S. Weiß, H. Schubert, L. Wesemann, *Chem. Commun.* **2019**, *55*, 10238–10240; c) J. D. Queen, J. C. Fettinger, P. P. Power, *Chem. Commun.* **2019**, *55*, 10285–10287.
[5] a) M. Ephritikhine, *Chem. Rev.* **1997**, *97*, 2193–2242; b) J. Okuda, *Coord. Chem. Rev.* **2017**, *340*, 2–9; c) M. Konkol, J. Okuda, *Coord. Chem. Rev.* **2008**, *252*, 1577–1591; d) M. Nishiura, Z. Hou, *Nat. Chem.* **2010**, *2*, 257–268.
[6] a) T. J. Marks, J. R. Kolb, *Chem. Rev.* **1977**, *77*, 263–293; b) B. Richter, J. B. Grinderslev, K. T. Møller, M. Paskevicius, T. R. Jensen, *Inorg. Chem.* **2018**, *57*, 10768–10780; c) M. Terrier, M. Visseaux, T. Chenal, A. Mortreux, *J. Polym. Sci. Part A* **2007**, *45*, 2400–2409; d) I. Palard, M. Schappacher, B. Belloncle, A. Soum, S. M. Guillaume, *Chem. Eur. J.* **2007**, *13*, 1511–1521; e) N. Barros, P. Mountford, S. M. Guillaume, L. Maron, *Chem. Eur. J.* **2008**, *14*, 5507–5518; f) D. Robert, M. Kondracka, J. Okuda, *Dalton Trans.* **2008**, 2667–2669; g) T. V. Mahrova, G. K. Fukin, A. V. Cherkasov, A. A. Trifonov, N. Ajellal, J.-F. Carpentier, *Inorg. Chem.* **2009**, *48*, 4258–4266; h) C. Schädle, A. Fischbach, E. Herdtweck, K. W. Törnroos, R. Anwander, *Chem. Eur. J.* **2013**, *19*, 16334–16341; i) S. Fadlallah, J. Jothieswaran, I. Del Rosal, L. Maron, F. Bonnet, M. Visseaux, *Catalysts* **2020**, *10*, 820; j) S. Fadlallah, J. Jothieswaran, F. Capet, F. Bonnet, M. Visseaux, *Chem. Eur. J.* **2017**, *23*, 15644–15654; k) S. Marks, J. G. Heck, M. H. Habicht, P. Oña-Burgos, C. Feldmann, P. W. Roesky, *J. Am. Chem. Soc.* **2012**, *134*, 16983–16986.
[7] a) G. G. Skvortsov, A. S. Shavyrin, T. A. Kovylina, A. V. Cherkasov, A. A. Trifonov, *Eur. J. Inorg. Chem.* **2019**, *2019*, 5008–5017; b) C. Schädle, C. Meermann, K. W. Törnroos, R. Anwander, *Eur. J. Inorg. Chem.* **2010**, *2010*, 2841–2852; c) F. Bonnet, C. E. Jones, S. Semlali, M. Bria, P. Roussel, M. Visseaux, P. L. Arnold, *Dalton Trans.* **2013**, *42*, 790–801; d) M. Visseaux, M. Terrier, A. Mortreux, P. Roussel, *Eur. J. Inorg. Chem.* **2010**, *2010*, 2867–2876; e) T. P. Seifert, T. S. Brunner, T. S. Fischer, C. Barner-Kowollik, P. W. Roesky, *Organometallics* **2018**, *37*, 4481–4487; f) X. Chen, S. Lim, C. E. Plečnik, S. Liu, B. Du, E. A. Meyers, S. G. Shore, *Inorg. Chem.* **2004**, *43*, 692–698; g) W. J. Evans, S. E. Lorenz, J. W. Ziller, *Chem. Commun.* **2007**,

4662–4664; h) W. J. Evans, J. M. Perotti, J. W. Ziller, *Inorg. Chem.* **2005**, *44*, 5820–5825.
[8] a) T. V. Fetrow, R. Bhowmick, A. J. Achazi, A. V. Blake, F. D. Eckstrom, B. Vlaisavljevich, S. R. Daly, *Inorg. Chem.* **2020**, *59*, 48–61; b) S. R. Daly, D. Y. Kim, Y. Yang, J. R. Abelson, G. S. Girolami, *J. Am. Chem. Soc.* **2010**, *132*, 2106–2107; c) S. R. Daly, B. J. Bellott, D. Y. Kim, G. S. Girolami, *J. Am. Chem. Soc.* **2010**, *132*, 7254–7255.
[9] a) T. Song, N. Liu, X. Tong, F. Li, X. Mu, Y. Mu, *Dalton Trans.* **2019**, *48*, 17840–17851; b) C. Qian, W. Nie, J. Sun, *Dalton Trans.* **1999**, 3283–3287.
[10] a) S. Y. Knjazhanskij, B. M. Bulychev, O. K. Kireeva, V. K. Belsky, G. L. Soloveichik, *J. Organomet. Chem.* **1991**, *414*, 11–22; b) S. Y. Knjazhanski, B. M. Bulychev, V. K. Belsky, G. L. Soloveichik, *J. Organomet. Chem.* **1987**, *327*, 173–179; c) V. K. Bel'skii, B. M. Bulychev, A. B. Erofeev, G. L. Soloveichik, *J. Organomet. Chem.* **1984**, *268*, 107–111; d) V. K. Belsky, A. B. Erofeev, B. M. Bulychev, G. L. Soloveichik, *J. Organomet. Chem.* **1984**, *265*, 123–133.
[11] K. D. Conroy, W. E. Piers, M. Parvez, *Organometallics* **2009**, *28*, 6228–6233.
[12] C. Schädle, D. Schädle, K. Eichele, R. Anwander, *Angew. Chem. Int. Ed.* **2013**, *52*, 13238–13242; *Angew. Chem.* **2013**, *125*, 13480–13484.
[13] C. Schädle, R. Anwander, *Eur. J. Inorg. Chem.* **2013**, *2013*, 3302–3306.
[14] a) B. L. L. Réant, S. T. Liddle, D. P. Mills, *Chem. Sci.* **2020**, *11*, 10871–10886; b) Z. Hou, Y. Zhang, M. Nishiura, Y. Wakatsuki, *Organometallics* **2003**, *22*, 129–135; c) N. S. Radu, T. D. Tilley, A. L. Rheingold, *J. Am. Chem. Soc.* **1992**, *114*, 8293–8295; d) N. S. Radu, T. Don Tilley, A. L. Rheingold, *J. Organomet. Chem.* **1996**, *516*, 41–49; e) A. D. Sadow, T. D. Tilley, *J. Am. Chem. Soc.* **2005**, *127*, 643–656; f) I. Castillo, T. D. Tilley, *Organometallics* **2001**, *20*, 5598–5605; g) N. S. Radu, F. J. Hollander, T. D. Tilley, A. L. Rheingold, *Chem. Commun.* **1996**, 2459–2460.
[15] a) W. S. Rees Jr., O. Just, H. Schumann, R. Weimann, *Angew. Chem. Int. Ed.* **1996**, *35*, 419–422; *Angew. Chem.* **1996**, *108*, 481–483; b) A. Pindwal, S. Patnaik, W. C. Everett, A. Ellern, T. L. Windus, A. D. Sadow, *Angew. Chem. Int. Ed.* **2017**, *56*, 628–631; *Angew. Chem.* **2017**, *129*, 643–646; c) J. Eppinger, M. Spiegler, W. Hieringer, W. A. Herrmann, R. Anwander, *J. Am. Chem. Soc.* **2000**, *122*, 3080–3096; d) K. Shinohara, H. Tsurugi, R. Anwander, K. Mashima, *Chem. Eur. J.* **2020**, *26*, 14130–14136; e) D. Werner, U. Bayer, D. Schädle, R. Anwander, *Chem. Eur. J.* **2020**, *26*, 12194–12205; f) A. Pindwal, K. Yan, S. Patnaik, B. M. Schmidt, A. Ellern, I. I. Slowing, C. Bae, A. D. Sadow, *J. Am. Chem. Soc.* **2017**, *139*, 16862–16874.
[16] M. N. Bochkarev, I. M. Penyagina, L. N. Zakharov, Y. F. Rad'kov, E. A. Fedorova, S. Y. Khorshev, Y. T. Struchkov, *J. Organomet. Chem.* **1989**, *378*, 363–373.
[17] a) J.-J. Maudrich, C. P. Sindlinger, F. S. W. Aicher, K. Eichele, H. Schubert, L. Wesemann, *Chem. Eur. J.* **2017**, *23*, 2192–2200; b) C. P. Sindlinger, W. Grahneis, F. S. W. Aicher, L. Wesemann, *Chem. Eur. J.* **2016**, *22*, 7554–7566; c) C. P. Sindlinger, A. Stasch, H. F. Bettinger, L. Wesemann, *Chem. Sci.* **2015**, *6*, 4737–4751.
[18] F. Diab, F. S. W. Aicher, C. P. Sindlinger, K. Eichele, H. Schubert, L. Wesemann, *Chem. Eur. J.* **2019**, *25*, 4426–4434.
[19] J.-J. Maudrich, F. Diab, S. Weiß, M. Widemann, T. Dema, H. Schubert, K. M. Krebs, K. Eichele, L. Wesemann, *Inorg. Chem.* **2019**, *58*, 15758–15768.
[20] G. Jeske, H. Lauke, H. Mauermann, P. N. Swepston, H. Schumann, T. J. Marks, *J. Am. Chem. Soc.* **1985**, *107*, 8091–8103.
[21] a) L. N. Bochkarev, V. M. Makarov, Y. N. Hrzhanovskaya, L. N. Zakharov, G. K. Fukin, A. I. Yanovsky, Y. T. Struchkov, *J. Organomet. Chem.* **1994**, *467*, C3–C5; b) M. N. Bochkarev, V. V. Khramenkov, Y. F. Rad'kov, L. N. Zakharov, Y. T. Struchkov, *J. Organomet. Chem.* **1991**, *408*, 329–334; c) M. N. Bochkarev, V. V. Khramenkov, Y. F. Rad'kov, L. N. Zakharov, Y. T. Struchjkov, *J. Organomet. Chem.* **1991**, *421*, 29–38; d) S.-M. Chen, J. Xiong, Y.-Q. Zhang, F. Ma, H.-L. Sun, B.-W. Wang, S. Gao, *Chem. Commun.* **2019**, *55*, 8250–8253.
[22] L. N. Bochkarev, O. V. Grachev, N. E. Molosnova, S. F. Zhiltsov, L. N. Zakharov, G. K. Fukin, A. I. Yanovsky, Y. T. Struchkov, *J. Organomet. Chem.* **1993**, *443*, C26–C28.
[23] F. G. N. Cloke, C. I. Dalby, P. B. Hitchcock, H. Karamallakis, G. A. Lawless, *Chem. Commun.* **1991**, 779–781.
[24] K. Zeckert, S. Zahn, B. Kirchner, *Chem. Commun.* **2010**, *46*, 2638–2640.
[25] L. N. Bochkarev, V. M. Makarov, L. N. Zakharov, G. K. Fukin, A. I. Yanovsky, Y. T. Struchkov, *J. Organomet. Chem.* **1995**, *490*, C29–C31.
[26] S. V. Klementyeva, C. Schrenk, M. Zhang, M. M. Khusniyarov, A. Schnepf, *Chem. Commun.* **2021**, *57*, 4730–4733.
[27] X. Wang, L. Andrews, *J. Am. Chem. Soc.* **2003**, *125*, 6581–6587.
[28] J. Vícha, J. Novotný, S. Komorovsky, M. Straka, M. Kaupp, R. Marek, *Chem. Rev.* **2020**, *120*, 7065–7103.
[29] C. P. Sindlinger, L. Wesemann, *Chem. Sci.* **2014**, *5*, 2739–2746.
[30] M. Widemann, K. Eichele, H. Schubert, C. P. Sindlinger, S. Klenner, R. Pöttgen, L. Wesemann, *Angew. Chem. Int. Ed.* **2021**, *60*, 5882–5889; *Angew. Chem.* **2021**, *133*, 5946–5953.
[31] a) R. E. White, T. P. Hanusa, *Organometallics* **2006**, *25*, 5621–5630; b) W. J. Evans, J. H. Meadows, A. G. Kostka, G. L. Closs, *Organometallics* **1985**, *4*, 324–326.
[32] M. Booij, B. J. Deelman, R. Duchateau, D. S. Postma, A. Meetsma, J. H. Teuben, *Organometallics* **1993**, *12*, 3531–3540.
[33] K. H. Den Haan, J. H. Teuben, *Chem. Commun.* **1986**, 682–683.
[34] C. Schädle, C. Maichle-Mössmer, K. W. Törnroos, R. Anwander, *Organometallics* **2015**, *34*, 2667–2675.
[35] a) F. Neese, *Wiley Interdiscip. Rev.: Comput. Mol. Sci.* **2018**, *8*, e1327; b) F. Neese, *Wiley Interdiscip. Rev.: Comput. Mol. Sci.* **2012**, *2*, 73–78.
[36] E. D. Glendening, J. K. Badenhoop, A. E. Reed, J. E. Carpenter, J. A. Bohmann, C. M. Morales, P. Karafiloglou, C. R. Landis, F. Weinhold, Theoretical Chemical Institute, University of Wisconsin, Madison, **2018**.
[37] a) K. H. Den Haan, Y. Wielstra, J. H. Teuben, *Organometallics* **1987**, *6*, 2053–2060; b) P. L. Watson, *Chem. Commun.* **1983**, 276–277; c) W. J. Evans, J. H. Meadows, A. L. Wayda, W. E. Hunter, J. L. Atwood, *J. Am. Chem. Soc.* **1982**, *104*, 2008–2014; d) R. Anwander, in *Lanthanides: Chemistry and Use in Organic Synthesis* (Ed.: S. Kobayashi), Springer Berlin Heidelberg, Berlin, Heidelberg, **1999**, pp. 1–61.
[38] C. J. Jameson, H. J. Osten, *J. Am. Chem. Soc.* **1985**, *107*, 4158–4161.
[39] A. Z. Voskoboynikov, I. P. Beletskaya, *New J. Chem.* **1995**, *19*, 723–726.
[40] M. Saito, H. Hashimoto, T. Tajima, M. Ikeda, *J. Organomet. Chem.* **2007**, *692*, 2729–2735.
[41] K. H. Den Haan, J. L. De Boer, J. H. Teuben, A. L. Spek, B. Kojic-Prodic, G. R. Hays, R. Huis, *Organometallics* **1986**, *5*, 1726–1733.
[42] L. Pu, M. M. Olmstead, P. P. Power, B. Schiemenz, *Organometallics* **1998**, *17*, 5602–5606.
[43] R. K. Harris, E. D. Becker, S. M. C. d. Menezes, R. Goodfellow, P. Granger, *Pure Appl. Chem.* **2001**, *73*, 1795–1818.
[44] a) Bruker, Madison, Wisconsin, USA, **2012**; b) G. M. Sheldrick, University of Göttingen, Germany, **2008**; c) L. J. Farrugia, *J. Appl. Crystallogr.* **1999**, *32*, 837–838; d) C. B. Hübschle, G. M. Sheldrick, B. Dittrich, *J. Appl. Crystallogr.* **2011**, *44*, 1281–1284; e) G. M. Sheldrick, *Acta Crystallogr. Sect. A* **2008**, *64*, 112–122.
[45] a) A. D. Becke, *Phys. Rev. A* **1988**, *38*, 3098–3100; b) J. P. Perdew, W. Yue, *Phys. Rev. B* **1986**, *33*, 8800–8802.
[46] S. Grimme, S. Ehrlich, L. Goerigk, *J. Comput. Chem.* **2011**, *32*, 1456–1465.
[47] a) F. Weigend, R. Ahlrichs, *Phys. Chem. Chem. Phys.* **2005**, *7*, 3297–3305; b) F. Weigend, *Phys. Chem. Chem. Phys.* **2006**, *8*, 1057–1065; c) B. Metz, H. Stoll, M. Dolg, *J. Chem. Phys.* **2000**, *113*, 2563–2569; d) D. Andrae, U. Häussermann, M. Dolg, H. Stoll, H. Preuß, *Theor. Chim. Acta* **1990**, *77*, 123–141.
[48] G. A. Zhurko, CHEMCRAFT (http://www.chemcraftprog.com).

Manuscript received: April 5, 2022
Accepted manuscript online: May 27, 2022
Version of record online: June 23, 2022